

SPG Mitteilungen Communications de la SSP

Auszug - Extrait

Progress in Physics (78)

Fitting a motor into a 1 nm³ cube

Samuel Stolz^{1,2}, Jan Prinz^{1,2}, Harald Brune², Roland Widmer¹, Oliver Gröning¹

¹ Empa, Swiss Federal Laboratories for Materials Science and Technology, 8600 Dübendorf

² Institute of Condensed Matter Physics, École Polytechnique Fédérale de Lausanne, 1015 Lausanne

This article has been downloaded from:

https://www.sps.ch/fileadmin/articles-pdf/2021/Mitteilungen_Progress_78.pdf

VI Directed motion is stimulated without applying a directed force nor a synchronized energy input to the system.

The unambiguous differentiation between forward and backward direction of motion, required from (II), implies that the motor cycles through at least 3 states (A, B and C, see fig. 1a)). Here, we might arbitrarily classify 'left-turning' as generating a sequence ...ABCABC... and 'right-turning' as generating ...ACBACB.... In contrast, a system switching between just two states (see top panel in fig. 1a)) represents a flip-flop and does not yield a time-ordered sequence. Requirements (V) and (VI) further entail the need of the system to exhibit inherent handedness, which distinguishes left-turning from right-turning, i.e., it must be chiral.

Design of our molecular motor

In our case the 3-fold symmetric (111) surface of the chiral intermetallic compound PdGa provides the basis to fulfill the requirements listed above. Specifically, it is the PdGa:A(-1-1-1)Pd₃ surface, labelled as Pd₃:A [9]. Figure 1b) schematically shows the top 3 atomic layers of the Pd₃:A surface, which is characterized by a hexagonal lattice of Pd trimers (large light-blue spheres). The chirality of the system and its relation to the scheme shown in fig. 1a) becomes more apparent if we concentrate on one atomic cluster, which is highlighted in the lower panels of fig. 1b) for Pd₃:A (m1) and its mirror image Pd₃:B (m2). One Pd trimer provides 3 energetically equivalent, yet distinguishable rotation states of the motor, thus fulfilling condition (V). The surrounding lower-lying Pd (blue) and Ga atoms (red) break any mirror symmetry. The chirality of this surface has been effectively transferred to adsorbed 9-ethynylphenantrene molecules, which trimerize into a prochiral pinwheel structure with 99% of them showing the same handedness (fig. 1c)) [8].

The cluster of 12 atoms in fig. 1b) constitutes the stator of our molecular motor. Its intrinsic chirality relaxes the structural requirements for the molecular rotor. That means, we can use very small and highly symmetrical molecules like acetylene to fulfill this role (see inset of fig. 2a)).

Probing the motion of the Pd₃:A - acetylene motor

Scanning tunneling microscopy (STM) images of individual acetylene molecules adsorbed on Pd₃:A at 77 Kelvin (K), reveal a peculiar bright, triangular signature of the molecule, as shown in fig. 2a). Instead of the expected 2-fold symmetry, a 3-fold symmetric structure centered on a Pd trimer is observed.

Cooling the system to 5 K and taking successive STM images reveals the nature of the acetylene observed at 77 K.

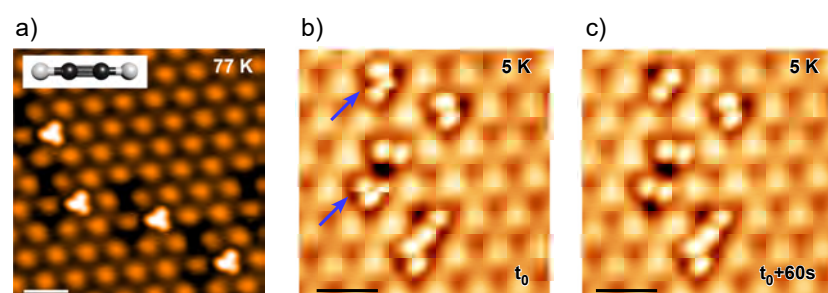


Figure 2: STM images of acetylene molecules adsorbed on the Pd₃:A surface recorded at a) 77 K and b) – c) 5 K. Scale bars correspond to 1 nm.

The molecules now appear dumbbell-shaped in 3 configurations rotated by 120° to each other [10]. Figure 2b) shows that during the relatively slow STM image acquisition, some of the acetylene molecules suddenly change their rotational configuration (marked by the blue arrows), as revealed in a subsequent STM image (fig. 2c)). Accordingly, the image at 77 K does not show static, but rapidly rotating molecules, such that the STM only detects a time-averaged image of all configurations at once. From the temperature dependence of the rotation rate, which we discuss later, we estimate that at 77 K the acetylene rotates with a frequency of a few MHz. The sequence of STM images in fig. 3a) shows the same acetylene molecule in its 3 distinguishable rotation configurations, which are labeled A, B, and C. Panel b) depicts schematic representations of the corresponding atomic configurations.

The conceptual setup of the STM experiment is illustrated in fig. 3c). Here, the atomic structure of the sample is measured by the tip of the STM brought into tunneling contact with the surface. At a fixed tip-position, any structural modification on the surface close-by will show up as a change in the tunneling current. The current-time series of fig. 3d) presents such structural modifications as it shows 23 current jumps between three well-defined values - each represents one of the rotational states of the acetylene molecule. The sequence of the rotational steps is perfectly ordered ...ABCABC..., which proves the highly unidirectional (counter-clockwise CCW) motion of the molecular rotor. It further shows that the rotation is not continuous like for a flywheel. Instead, the jumps happen theoretically within a few picoseconds and are followed by much longer rest periods. By determining the number of CCW (n_{CCW}) and clockwise (CW) rotation events (n_{CW}), we can quantify the directionality $d = (n_{CCW} - n_{CW}) / (n_{CCW} + n_{CW})$ of the motor. Under ideal conditions, we could establish that d is above 97% with 2σ confidence, which means that CCW rotation events is 100 times more likely than CW ones.

Although it seems natural to attribute this high degree of directionality to the handedness of the PdGa stator, also the STM tip introduces handedness into the system due to its usually non-symmetric shape and position on the substrate. Indeed, the chirality of the STM tip has been deemed responsible for low degrees of directionality of 3 - 5 % in surface anchored molecular rotors [11].

In order to clarify the role of the tip-position on the molecular rotation, we have measured 6400 time-series such as the one shown in fig. 3d) distributed on a 80 × 80 point grid spanning an area of 1 × 1 nm². At 5 K and an applied tip voltage of 10 mV at 100 pA current, we observe a jump frequency of a few Hz, which is largely independent of the tip-position as can be seen from fig. 4a). The region where the rotation is detected has the same shape as the residence map at 77 K (see fig. 4b)), confirming its origin to be the time-averaged image of a fast rotating acetylene. The map of the jump sequence, displayed in fig. 4c), shows a directionality (absolute value of the jump sequence) close to 1 - independent of the tip-position. The color of the map denotes whether the jump sequence is ascending (red) or descending (blue). The agreement of the experimental map with the simulated pattern in fig. 4d) (which assumes exclusively CCW rotation) proves that the direction of the rotation is independent on

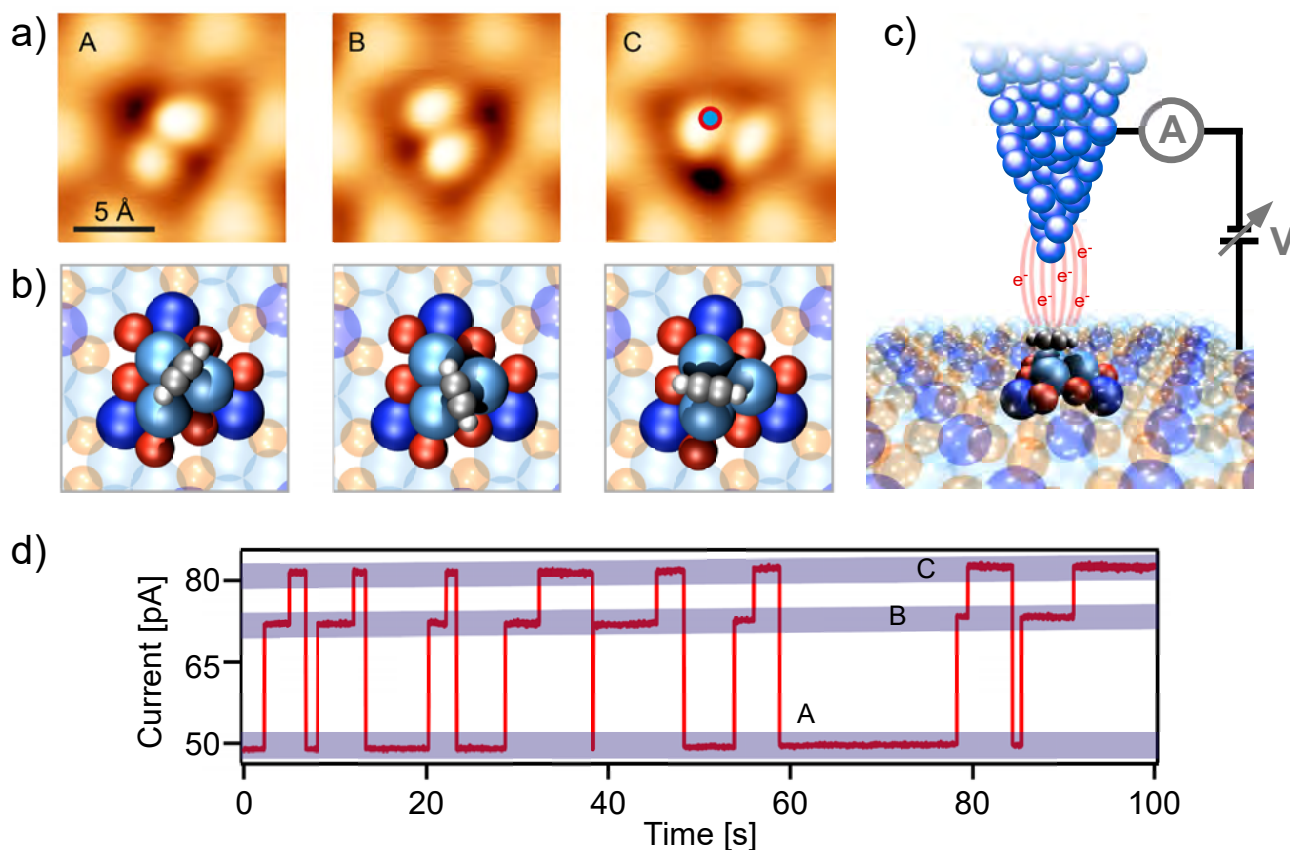


Figure 3: a) STM images and b) the corresponding atomistic models of one acetylene molecule on the Pd₃:A surface in its three equivalent, 120° rotated states. c) Schematic illustration of the experimental setup to probe and drive the acetylene on Pd₃:A molec-

ular motor with an exemplary experimental current-time sequence in d). A time-lapse movie of the rotation can be found here <https://www.youtube.com/watch?v=j3mNH2vXTqA&t=5s>

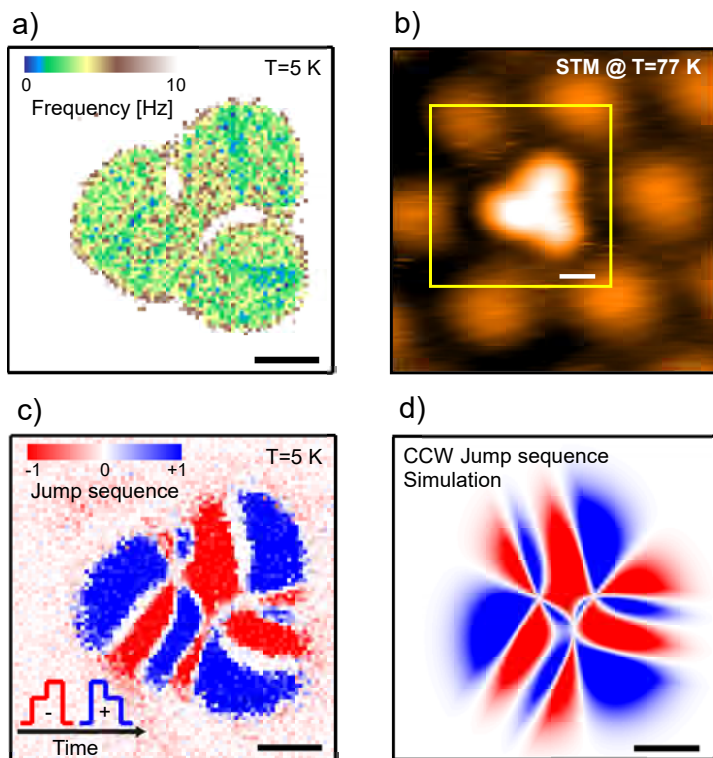


Figure 4: Influence of the STM-tip-position relative to the acetylene molecular motor on a) the rotation frequency and c) the jump sequence at 5 K. b) The STM signature of a fast rotating acetylene molecule on the Pd₃:A surface at 77 K. The simulated jump sequence map in d), assuming only counter-clockwise rotation events. Scale bars correspond to 2 Å.

the STM-tip and confirms that the handedness of the stator dictates the direction of the motor rotation.

Powering the molecular motor

Up to this point, we have only mentioned the temperature dependence of the rotation. Figure 5a) shows the quantitative dependence of frequency and directionality on temperature. Below 15 K, the rotation frequency of about 5 Hz is temperature-independent and exhibits a directionality close to 1. Above 15 K, the frequency increases with an Arrhenius-like characteristics from which we deduce an activation energy around 25 meV. Concomitantly with the onset of the thermally activated rotations, the directionality drastically deteriorates. The decrease is well described by the assumption that the directionality of the constant 5 Hz component remains close to 1 for all temperatures, whereas the additional temperature-induced rotations are random. The latter observation is not surprising as substrate, molecule and STM-tip are in thermal equilibrium during the measurement and a consistently directional thermal motion would violate the 2nd law of thermodynamics as it represents a negative change of entropy (ΔS).

The voltage dependence of frequency and directionality, presented in fig. 5b), shares some similarities with the temperature dependence. Above some critical voltage of about 35 mV, we observe an exponential increase of the rotation frequency for both polarities from a voltage-independent base frequency. Contrary to the temperature dependence, this voltage-driven frequency increase is not accompanied by an immediate decrease in the directionality. Especially at voltages close to 35 mV the majority of voltage-induced

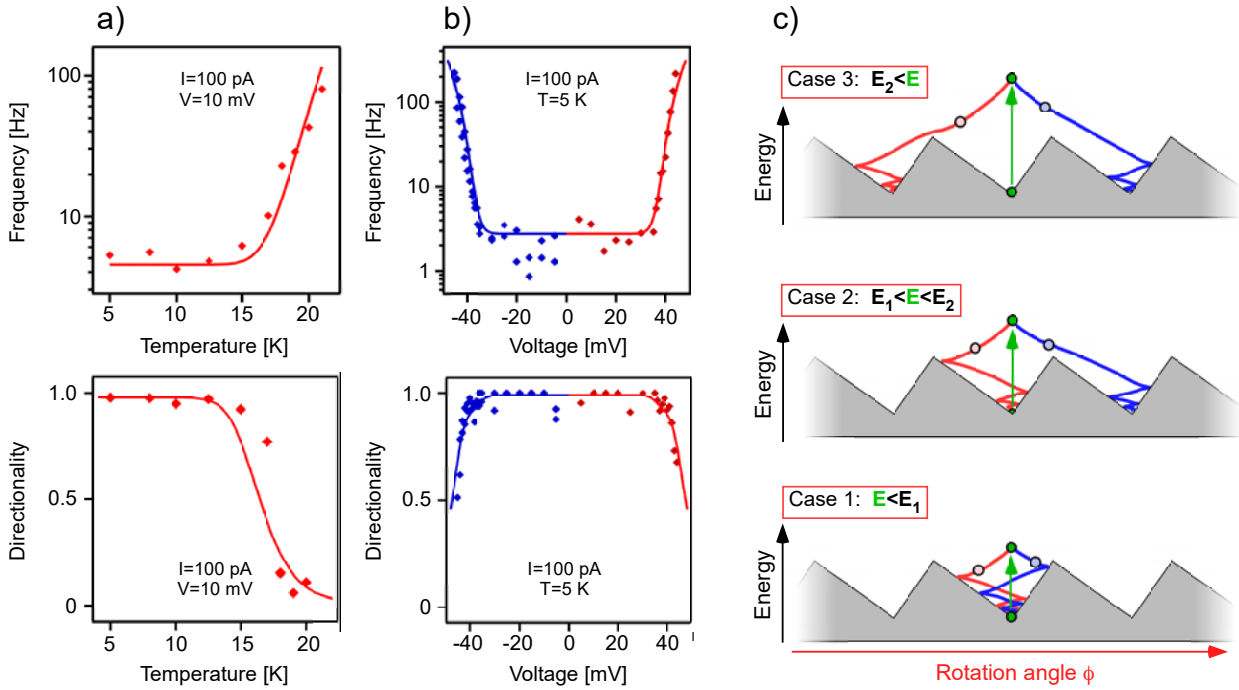


Figure 5: The dependence of our molecular motor's rotation frequency and directionality on a) temperature and b) applied bias voltage. In c) the three cases for energy transferred to the acety-

lene molecule via inelastic electron tunneling are sketched. For a detailed description of the three cases, we refer to the text.

rotations remain unidirectional. With increasing voltage the direction of the rotations, however, becomes more and more random.

Friction and directionality of the motor

In order to interpret these findings, let us examine the role of dissipation in this system. If we think of an ideal heat engine operating between two finite, non-zero temperatures, Sadi Carnot showed that we could not expect 100% efficiency. However, provided we have energy sources of higher quality, e.g., electricity, the Carnot efficiency is not the limiting factor anymore and electric motors with efficiencies of up to 99.05% have been realized [12].

Although we would ideally like to completely eliminate dissipation losses, they are indispensable to achieve unidirectional motion. This fact is illustrated in fig. 5c) by displaying the sequence of dissipative trajectories (according to Langevin dynamics [13,14]) of the acetylene molecule in its asymmetric rotation potential. From the linear dependence of the voltage-activated rotations with the STM tunneling current, we conclude that a rotation step is a single electron event. That means, a single electron excites the molecule by transferring part of its energy through inelastic tunneling to its rotational degree of freedom. Because of friction, the initial rotational energy needs to exceed the potential barrier by some margin to overcome it. The bottom panel of fig. 5c) illustrates the situation when the initial energy is below the critical value of E_1 and no rotation step is possible. Above E_1 (middle panel of fig. 5c)) it is possible for the molecule to overcome the barrier on the steeper side and to perform a rotation step in the CCW direction (blue). CW rotation steps (red) are not occurring because the molecules loses too much kinetic energy on the longer trajectory to the potential maximum. If, however, the initial energy exceeds a second threshold E_2 these latter jumps in the 'wrong' direction become possible, too (see top panel of fig. 5c)). Consequently, highly directional motion of the rotor only occurs if the ex-

citation energy of the system is between E_1 and E_2 . The values of the threshold energies E_1 and E_2 combine information of the potential height, its asymmetry R (defined as the ratio of the rotation path length from the minimum of the potential to its left (CCW) and right (CW) maximum) and the viscous dissipation coefficient λ .

By matching the experimental voltage dependence to a classical Langevin model, we obtain threshold energies of $E_1 = 39$ meV and $E_2 = 44$ meV, which is significantly higher than the potential barrier height of 25 meV. Accordingly, the energy dissipation at 5 K amounts to $\lambda = 1.6 \cdot 10^{-33}$ kgm²/s. At higher temperatures, energy dissipation becomes less efficient, such that at 20 K we find the energy thresholds reduced to $E_1 = 34$ meV and $E_2 = 38$ meV, which translates to a dissipation coefficient of about $\lambda = 1.0 \cdot 10^{-33}$ kgm²/s. The asymmetry ratio R is temperature-independent and, with a value between 1.25 and 1.5, surprisingly small. For comparison, in fig. 5c) the potential has an $R = 2$.

The quantum nature of the motor

So far, we treated the rotation of the acetylene molecule classically, without much justification. As shown in fig. 6a) solving the Schrödinger equation of the system reveals a strong quantization of the rotation modes to 4 energy levels. Accordingly, the classical approximation is only a very coarse approximation to describe the system. The significant quantum character of the rotation, however, also holds the key to understand the constant, sub-threshold rotation frequency shown in fig. 5a) and 5b). Such constant rates have been frequently observed in surface diffusion and reaction processes [15–19] and are generally attributed to quantum tunneling. A feature of this effect is the exponential dependence of the reaction rate with the mass or, in this case, the moment of inertia of the tunneling system. Figure 6b) shows current-time series when the hydrogen atoms of the acetylene are replaced with deuterium (singly deuterated C₂HD and doubly deuterated C₂D₂). Although the

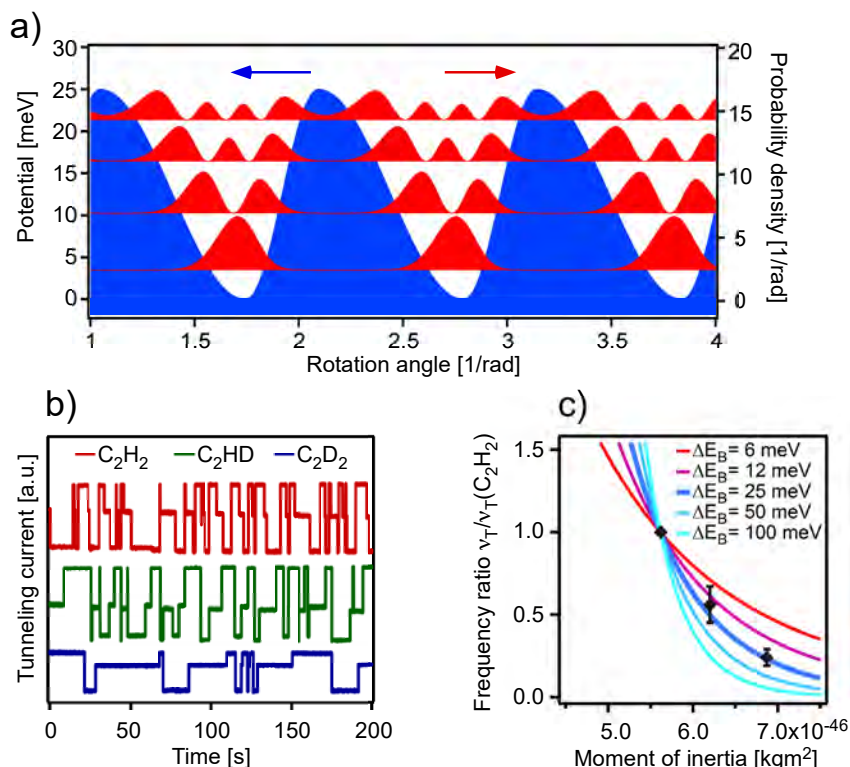


Figure 6: a) Illustration of the four rotation modes and their respective probability density (red) of the acetylene molecule within a potential with 25 meV energy barriers (blue). b) Experimental current-time series of acetylene molecules containing different amounts of deuterium. c) Comparison of the relative, experimental tunneling frequencies of C₂H₂, C₂HD and C₂D₂ (black markers, shown as ratio to the C₂H₂ frequency $\nu_T(C_2H_2)$) and the simulated ones in the WKB approximation for different potential barrier heights.

moment of inertia increases just by 10% for each deuterium replacing a hydrogen, the rotation frequency is reduced by a factor of 2. This exponential behavior of the tunneling rate is consistent with tunneling through a 25 meV barrier in the WKB (Wenzel-Kramers-Brillouin) approximation [20] as shown in fig. 6c).

Outlook

The feature rendering this particular rotor unique is that also in the tunneling regime the rotation is highly directional ($d > 97\%$). Therefore, also in the tunneling case energy dissipation needs to be an essential ingredient to understand the system. The atomistic details how the system is pushed out of the equilibrium and how friction enters into the tunneling motion are not understood at this point. Yet, the well-defined structure of the system with only 16 atoms (12 of the PdGa stator and 4 of the acetylene rotor, see. fig. 3b)) and its accessibility to detailed experimental characterization render it ideal to understand the role of:

- i) Electron-phonon coupling in inelastic electron-tunneling induced motion
- ii) Energy dissipation and friction on the molecular level
- iii) Non-equilibrium, dissipative quantum tunneling

We hope that in the future a concerted effort of theoretical and experimental investigations will shed more light into these important research questions, such that this 'world smallest motor' will be more than the realization of a nanotechnological 'curiosity'.

Acknowledgements

This contribution to the *SPG Mitteilungen* is based on the research article "Molecular motor crossing the frontier of classical to quantum tunneling motion" by S. Stolz et al. published in the *Proceedings of the National Academy of Sciences of the United States of America* **117**(26), 14838 (2020). The financial support for this research from the Swiss National Science Foundation under the grants 200021-129511 and 200021-159690 is gratefully acknowledged.

Bibliography

- [1] Feynman, R. P., Leighton, R. B. & Sands, M. *The Feynman Lectures on Physics*. vol. 1 (Addison-Wesley, 1963).
- [2] Newman, T. H., Williams, K. E. & Pease, R. F. W. High resolution patterning system with a single bore objective lens. *J. Vac. Sci. Technol. B Microelectron. Process. Phenom.* **5**, 88–91 (1987).
- [3] Feynman, R. Infinitesimal machinery. *J. Microelectromechanical Syst.* **2**, 4–14 (1993).
- [4] Nagatashi Koumura, R. W. J. Z., Richard A. van Delden, N. H. & Ben L. Feringa. Light-driven monodirectional molecular motor. *Nature* **401**, 152–155 (1999).
- [5] Kelly, T. R., De Silva, H. & Silva, R. A. Unidirectional rotary motion in a molecular system. *Nature* **401**, 150–152 (1999).
- [6] Salma Kassern, T. van L., Anouk S. Lubbe, M. R. W. & Ben L. Feringa, D. A. L. Artificial molecular motors. *Chem Soc Rev* **46**, 2592–2621 (2017).
- [7] Stolz, S., Gröning, O., Prinz, J., Brune, H. & Widmer, R. Molecular motor crossing the frontier of classical to quantum tunneling motion. *Proc. Natl. Acad. Sci.* **117**, 14838–14842 (2020).
- [8] Stolz, S. et al. Near-enantiopure trimerization of 9-Ethynylphenanthrene on a chiral metal surface. *Angew. Chem. Int. Ed.* **59**, 18179–18183 (2020).
- [9] Prinz, J. et al. Isolated Pd sites on the intermetallic PdGa(111) and PdGa(-1-1-1) model catalyst surfaces. *Angew. Chem.* **124**, 9473–9477 (2012).
- [10] Prinz, J. et al. Adsorption of Small Hydrocarbons on the Three-Fold PdGa Surfaces: The Road to Selective Hydrogenation. *J. Am. Chem. Soc.* **136**, 11792–11798 (2014).
- [11] Heather L. Tierney, C. J. M., April D. Jewell, A. E. B., Allister F. McGuire, N. K. & E. Charles H. Sykes. Experimental demonstration of a single-molecule electric motor. *Nat. Nanotechnol.* **6**, 625–629 (2011).
- [12] ABB reaches 99.05% efficiency, the highest ever recorded for a synchronous motor - ABB Conversations. <https://www.abb-conversations.com/2017/07/abb-motor-sets-world-record-in-energy-efficiency/>.
- [13] Hänggi, P. & Marchesoni, F. Artificial Brownian motors: Controlling transport on the nanoscale. *Rev Mod Phys* **81**, 387–442 (2009).
- [14] Astumian, R. D., Mukherjee, S. & Warshel, A. The physics and physical chemistry of molecular machines. *ChemPhysChem* **17**, 1719–1741 (2016).
- [15] Heinrich, A. J., Lutz, C. P., Gupta, J. A. & Eigler, D. M. Molecule cascades. *Science* **298**, 1381–1387 (2002).
- [16] Lauthon, L. J. & Ho, W. Direct observation of the quantum tunneling of single hydrogen atoms with a scanning tunneling microscope. *Phys. Rev. Lett.* **85**, 4566–4569 (2000).
- [17] Stroschio, J. A. & Celotta, R. J. Controlling the dynamics of a single atom in lateral atom manipulation. *Science* **306**, 242–247 (2004).
- [18] Nacci, C. et al. Current versus temperature-induced switching in a single-molecule tunnel junction: 1,5 cyclooctadiene on Si(001). *Nano Lett.* **9**, 2996–3000 (2009).
- [19] Lin, C., Durant, E., Persson, M., Rossi, M. & Kumagai, T. Real-space observation of quantum tunneling by a carbon atom: flipping reaction of formaldehyde on Cu(110). *J. Phys. Chem. Lett.* **10**, 645–649 (2019).
- [20] Prager, M. & Heidemann, A. Rotational tunneling and neutron spectroscopy: A compilation. *Chem. Rev.* **97**, 2933–2966 (1997).